

# Krypton Tagging Velocimetry for Use in High-Speed Ground-Test Facilities

N. J. Parziale\*

*Stevens Institute of Technology, Hoboken, NJ 07030, USA*

M. S. Smith<sup>†</sup> E. C. Marineau<sup>‡</sup>

*AEDC White Oak, Silver Spring, MD 20903, USA*

In this work, we present the excitation strategy, experimental setup, and results of an implementation of krypton tagging velocimetry (KTV) as applied to an underexpanded jet of three mixtures. We demonstrate that the KTV technique can be employed with gas mixtures of relatively low krypton concentration (0.5% Kr/99.5% N<sub>2</sub>) and conclude that the KTV technique shows promise as a velocimetry diagnostic with krypton as an inert, dilute, long-lifetime tracer in gas-phase flows.

## Nomenclature

$\Delta x$	Distance traversed by metastable Kr, (m)
$\Delta t$	Time between the write and read laser Q-switch pulses, (s)
$V$	Velocity, (m/s)
$D$	Diameter, (m)
$M$	Mach number, (-)
$X_i$	Mole fraction of species i, (-)
$\gamma$	Ratio of specific heats, (-)
$W$	Mean molar mass of mixture, (g/mol)
$P$	Pressure, (Pa)
$\rho$	Density, (kg/m <sup>3</sup> )
$c$	Sound speed, (m/s)

### Subscript

$j$	jet
$w$	at the write location

## I. Introduction

Velocimetry techniques for use in high-speed wind-tunnel facilities are of interest to the US Air Force to study flow fields for the purposes of test and evaluation. These investigations are intended to further the understanding of the fundamental flow physics that influence macro-scale behavior of test articles with the goal of assisting flight-vehicle development. Researchers have developed various forms of velocimetry techniques; for examples, see the handbook edited by Tropea et al.<sup>1</sup> In that hand book, there is a chapter<sup>2</sup> that describes the basics of tagging velocimetry, which will be the focus of this work.

\*Assistant Professor, Mechanical Engineering, Castle Point on Hudson, Hoboken, New Jersey, 07030, AIAA Member.

<sup>†</sup>Senior Research Engineer, Aerospace Testing Alliance, Silver Spring, MD 20903, Senior AIAA Member.

<sup>‡</sup>Lead Aerospace Technologist, AEDC White Oak, Silver Spring, MD 20903, AIAA Member.

## II. Review and Motivation for Exploration of Krypton as a Tracer

The general methodology of tagging velocimetry is similar to observing the translation of dye that has been seeded into the flow as seen in the National Committee for Fluid Mechanics Films:<sup>3</sup> insert a tracer and observe the tracer as the flow field evolves. Different constituents can be used as the tagging medium in high-speed gas flows; and, each has advantages and disadvantages.

Oxygen may be used as an unseeded tracer in air and O<sub>2</sub> flows, or possibly partially dissociated CO<sub>2</sub> flows. The RELIEF technique<sup>4–8</sup> utilizes vibrationally-excited O<sub>2</sub> as a tracer and has a lifetime that is a function of the vibrational relaxation time. Researchers report the use of a dye laser and an ArF laser to implement RELIEF. Additionally, researchers have tagged flows by photosynthesis of ozone. Subsequently, the ozone is photodissociated and LIF is imaged from the resulting O<sub>2</sub>.<sup>9–11</sup> The ozone tracer can have a lifetime on the order of seconds.

Nitrogen can be used as an unseeded tracer in air and N<sub>2</sub> flows. In Michael et al.,<sup>12</sup> the tracer was created by nonlinear excitation and dissociation of nitrogen with a femtosecond laser. The position is recorded by imaging the emission of the recombining nitrogen atoms. In that work, researchers report an effective lifetime on the order of 10 μs.

Nitric oxide (NO) is an attractive candidate as a tracer for reasons including its long lifetime (order 1–10 ms in the absence of polyatomic molecules) and ease of in-situ-production/seeding. The APART technique<sup>13–15</sup> entails the photosynthesis of NO from N<sub>2</sub> and O<sub>2</sub> by an ArF excimer laser, so it may be applied in air. A dye-laser is used to induce fluorescence from the tagged NO. Researchers have utilized the photodissociation of seeded (CH<sub>3</sub>)<sub>3</sub>CONO,<sup>16</sup> NO<sub>2</sub><sup>17–24</sup> or N<sub>2</sub>O<sup>25</sup> to produce NO, and subsequently image LIF for time-of-flight velocimetry. Additionally, researchers have also utilized direct NO seeding for velocimetry.<sup>26–30</sup> Furthermore, researchers have performed experiments in shocktunnels with prescribed shocktube mixtures (≈99% N<sub>2</sub> ≈1% O<sub>2</sub>) to create ≈1% NO in the free stream for velocimetry.<sup>31–33</sup> It should be noted that the VENOM technique<sup>18–21,30</sup> is also capable of simultaneous temperature measurements.

Other tracers include iodine,<sup>34,35</sup> acetone,<sup>36–38</sup> and the hydroxyl group<sup>39–41</sup> among others.<sup>42–45</sup> These schemes generally require seeding or in-situ production of the tracer.

The fundamental strength of KTV is that the tracer (metastable krypton) is nominally<sup>a</sup> inert; this is in contrast to other tracers that represent the current state of the art. The non-reactive nature of krypton as a tracer will enable the technique to be employed in a wide variety of flows because the seeded krypton atoms are nominally independent of chemical processes that may occur in the bulk flow that is being investigated. Because of this flexibility, KTV demonstrates the potential to broaden the usefulness of tagging velocimetry with new applications in the study of hypersonic flow physics, particularly in non-equilibrium gas-phase flows. Furthermore, Hsu et al.<sup>47</sup> review the benefits of using Kr as a tagging medium, namely: the atomic structure is well known, and relative to other noble gases, two-photon excitation is accessible with commercially available laser and optical components. Moreover, Kr gas-bottle cost is appropriate for laboratory-scale efforts.

KTV may prove particularly useful where the composition of the flow field of interest is difficult to prescribe. For example, in high-enthalpy aerodynamics work, it is typical for researchers to investigate thermo-chemical/fluid-mechanic interaction by studying and comparing flows with gases that are more thermo-chemically active (e.g., CO<sub>2</sub>, air) and less thermo-chemically active (e.g., N<sub>2</sub>). It may be possible for krypton to be used as a tracer in CO<sub>2</sub>, air, or N<sub>2</sub>, so the researcher would not have to change velocimetry diagnostics to investigate different gasses about the same body for studies of thermochemical effects on aerodynamics<sup>48–50</sup> and boundary-layer instability and transition.<sup>51–53</sup>

A similar potential for exists for combustion flows, but as Miles and Lempert<sup>7</sup> indicate, one “limitation [of tagging velocimetry] has to do with the lifetime of the tagged molecules. Of particular importance are collisions with polyatomic molecules such as water, carbon dioxide, and in combustion applications, fuels such as methane and other hydrocarbons.” However, the prospects of using KTV in flows with polyatomic molecules is promising. Buxton et al.<sup>54</sup> and Hsu et al.<sup>47</sup> have utilized Kr for PLIF work in combustion

<sup>a</sup>We use the term nominally because the first ionization energy of Kr is 14 eV. This is in comparison to the creation of NO<sup>+</sup> by N + O + 2.8 ev = NO<sup>+</sup> + e, which is considered to be the most important role of ionization in air.<sup>46</sup>

environments with Kr seeding mole fractions of  $\approx 1 - 4\%$ . These researchers also note that the seeding mole fractions of 1% “avoided disturbance of the flame.”

Researchers report the metastable state has a lifetime on the order of 1-10 s.<sup>55-57</sup> However, in those experiments, the gas pressure is low relative to the gas pressure to be used in flows of interest to aerothermodynamics research. This results in a shorter expected lifetime of the metastable Kr tracer in current applications, and is a topic of current research.

We focus our efforts on tagging velocimetry with krypton as an inert tracer, as suggested by Mills et al.<sup>58</sup> and Balla and Everhart.<sup>59</sup> Mills et al.<sup>58</sup> proposed that tagging velocimetry could be performed as follows:

1. *Write* tracer line by two-photon excitation,  $6p[3/2]_2 \leftarrow 4p^6(^1S_0)$  (193 nm) with an ArF laser
2. *Decay* to metastable state,  $5s[3/2]_2 \leftarrow 6p[3/2]_2$  (427.4 nm)
3. *Excite*  $5p[5/2]_3$  level by  $5p[5/2]_3 \leftarrow 5s[3/2]_2$  (811.3 nm) with a diode laser
4. *Read* spontaneous emission of  $5s[3/2]_2 \leftarrow 5p[5/2]_3$  (811.3 nm) transitions with a camera positioned normal to the flow.

This strategy would permit time of flight velocimetry measurements. However, we are not restricted to the creation of metastable Kr atoms with an ArF laser through the  $5s[3/2]_2 \leftarrow 6p[3/2]_2 \leftarrow 4p^6(^1S_0)$  transition strategy, which may necessitate the need for an ArF laser. For example, Narayanaswamy et al.<sup>60</sup> used two-photon excitation of the  $5p[3/2]_2$  level with a dye laser and subsequent decay via the  $5s[3/2]_1 \leftarrow 5p[3/2]_2$  and  $5s[3/2]_2 \leftarrow 5p[3/2]_2$  transitions in Kr planar laser induced fluorescence (PLIF) work for flow visualization and scalar imaging of an underexpanded jet of 100% krypton; this is the write-excitation strategy we will use in this work.

Given that the krypton may be seeded into the flow in dilute concentrations, the thermo-physical properties of the flow are nominally unchanged. Estimates of the effect of dilute krypton concentrations on the transport properties can be done using Cantera<sup>61</sup> with the appropriate thermodynamic data.<sup>62-64</sup> For example, if N<sub>2</sub> is seeded with 1% Kr at 300 K at 1 atm, the Reynolds, Prandtl, Lewis, and Peclet numbers and the ratio of specific heats are changed by  $\approx 0.1 - 0.3\%$ . Additionally, the Schmidt number of the tagged krypton is approximately the same ( $\approx 1$ ) as other tagging schemes utilizing nitrogen, oxygen, or nitrogen oxide; so, there is little relative diffusional effect of KTV versus the other gas-phase tagging schemes.

In this work, we present the krypton transition strategy, experimental setup, and results of an implementation of krypton tagging velocimetry (KTV) as applied to an underexpanded jet of three mixtures. The KTV results are reduced and compared to an appropriate correlation of historical data.

### III. Experimental Setup

To use krypton as a tracer in a gas flow field, pulsed tunable lasers can be used to excite and/or induce fluorescence of Kr atoms that have been seeded into the flow for the purposes of position tracking. An energy level diagram for the proposed KTV scheme is presented as Fig. 1 (left). The excitation/emission strategy is as follows:

1. *Write* tracer line by two-photon excitation of  $5p[3/2]_2 \leftarrow 4p^6(^1S_0)$  (214.7 nm)
2. *Decay* to metastable states  $5s[3/2]_1 \leftarrow 5p[3/2]_2$  (819.0 nm) and  $5s[3/2]_2 \leftarrow 5p[3/2]_2$  (760.2 nm)
3. *Excite*  $5p[3/2]_2$  level by  $5p[3/2]_2 \leftarrow 5s[3/2]_2$  transition with laser sheet (760.2 nm)
4. *Read* spontaneous emission of  $5s[3/2]_1 \leftarrow 5p[3/2]_2$  (819.0 nm) and  $5s[3/2]_2 \leftarrow 5p[3/2]_2$  (760.2 nm) transitions with a camera positioned normal to the flow.

Miller<sup>65</sup> reports two-photon excitation of the  $5p[3/2]_2$  level in Kr at 214.7 nm ( $5p[3/2]_2 \leftarrow 4p^6(^1S_0)$  transition). The same work reports that a branching fraction for two decay transitions,  $5s[3/2]_1 \leftarrow 5p[3/2]_2$  (819.0 nm) and  $5s[3/2]_2 \leftarrow 5p[3/2]_2$  (760.2 nm), of approximately 27% and 73%, respectively. We choose the  $5s[3/2]_2 \leftarrow 5p[3/2]_2$  (760.2 nm) transition for read-excitation because of the favorable branching fraction<sup>47</sup> to obtain a strong signal to noise ratio. The  $5s[3/2]_1 \leftarrow 5p[3/2]_2$  and  $5s[3/2]_2 \leftarrow 5p[3/2]_2$  transitions occur on a time-scale of approximately 20-35 ns.<sup>66-69</sup>

To demonstrate the KTV technique, an underexpanded jet is used as the flow field. The jet-orifice diameter is  $D_j = 2$  mm. This jet was exhausted into a test cell, which was continuously evacuated to maintain a pressure of approximately 7 torr. Well-mixed gas mixtures for the jet were created in a pressure vessel. A gas-pressure regulator was used to control the effective plenum pressure of the underexpanded jet, and a high-speed solenoid (ITT S31 series) was used to pulse the jet. There is optical access to the test cell through three fused silica windows; two windows permit the read and write beams to enter and leave the test cell, and the third window is positioned at  $90^\circ$  to the other two windows to permit imaging.

The write excitation was performed with a frequency doubled Continuum ND6000 Dye Laser, which was pumped with 400 mJ/pulse at 355 nm from a frequency tripled Continuum PR8010 Nd:YAG laser. The dye was Coumarin 440 and supplied by Exciton. Frequency doubling of the dye laser output (429.4 nm) was performed with an Inrad BBO-C ( $65^\circ$ ) crystal placed in a Inrad 820-360 gimbal mount. The 214.7 nm and 429.4 nm beams are separated with a Pellin-Broca prism; the 429.4 nm beam is sent to a beam dump and the 214.7 nm beam is focused to a narrow waist ( $\approx 40 \mu\text{m}$  in diameter) in the test section over the jet with a 600 mm fused silica lens (Fig. 1 center, Fig. 2). This setup resulted in approximately 1 mJ/pulse, with a wavelength of 214.7 nm, a linewidth of approximately  $10 \text{ cm}^{-1}$ , and a repetition rate of 10 Hz.

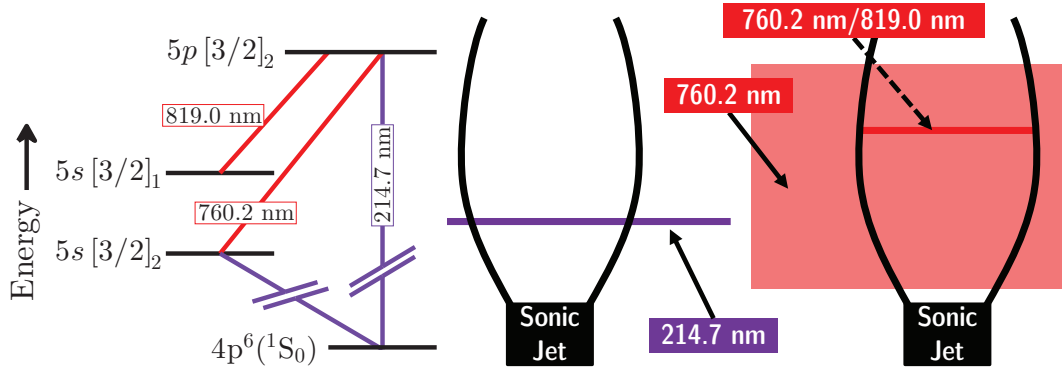


Figure 1. *Left:* Energy level diagram for KTV. *Center:* Schematic of the jet and the write line, which is purple and indicated by the solid arrow marking 214.7 nm. *Right:* Schematic of the jet, and the read-excitation sheet which is red and indicated by the solid arrow marking 760.2 nm. Additionally on the right, is the spontaneous emission line from the tagged, excited, and advected Kr atoms, which is indicated by the dashed arrow marking 760.2 nm/819.0 nm emission. The object plane of the intensified camera is parallel to the page and coincident with the read sheet.

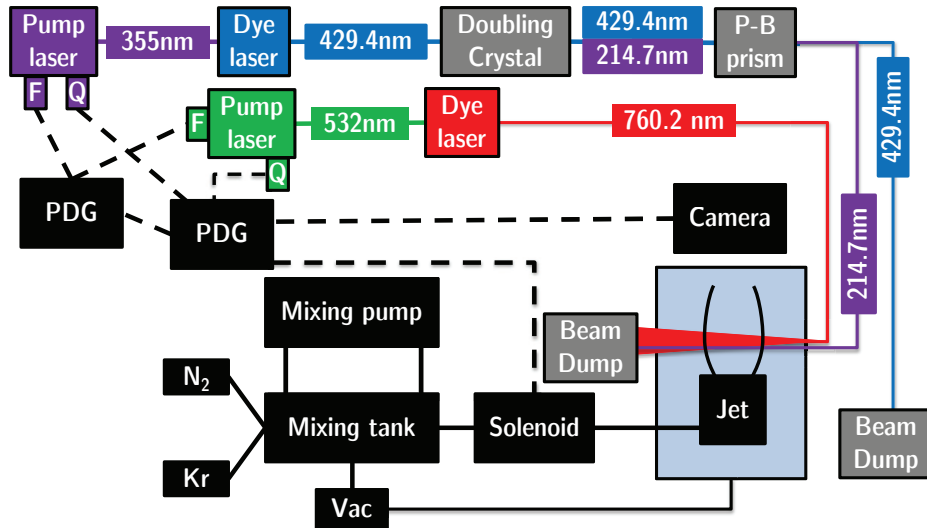


Figure 2. Block diagram of experimental setup. Dashed lines indicate wiring. Solid lines indicate plumbing. valves are not indicated. PDG is pulse delay generator. P-B prism is Pellin-Broca prism. F is flashlamp. Q is Q-switch. Vac is vacuum. Not to scale or indicative of plane.

**Table 1.** Conditions at the write location of the underexpanded jet for each of the three cases.  $X_{\text{Kr}}$  is the Kr mole fraction,  $X_{\text{N}_2}$  is the  $\text{N}_2$  mole fraction,  $\gamma_w$  is the ratio of specific heats,  $W$  is the mean molar mass of the mixture.  $P_R$  is the effective reservoir pressure.  $P_w$ ,  $\rho_w$ ,  $V_w$ ,  $M_w$ ,  $\text{Re}_w^{\text{unit}}$ , and  $\text{Pr}_w$  are the static pressure, density, velocity, Mach number, unit Reynolds number, and Prandtl number calculated per the empirical fit in Crist et al.<sup>70</sup>

Case	$X_{\text{Kr}}$ (-)	$X_{\text{N}_2}$ (-)	$P_R$ (kPa)	$W$ (g/mol)	$P_w$ (Pa)	$\rho_w$ (kg/m <sup>3</sup> )	$V_w$ (m/s)	$M_w$ (-)	$\gamma_w$ (-)	$\text{Re}_w^{\text{unit}}$ (1/m)	$\text{Pr}_w$ (-)
1, Fig. 3	1.000	0.000	240	83.8	491	0.200	507	5.72	1.67	56.7e6	0.667
2, Fig. 4	0.050	0.950	180	30.8	345	0.027	707	5.01	1.41	79.0e6	0.700
3, Fig. 5	0.005	0.995	180	28.3	340	0.024	714	5.00	1.40	79.7e6	0.708
4	0.000	1.000	180	28.0	340	0.023	715	5.00	1.40	79.8e6	0.709

The read excitation was performed with a Continuum ND60 Dye Laser, which was pumped with approximately 250 mJ/pulse at 532 nm from a frequency doubled Continuum NY82S-10 Nd:YAG laser. The dye was LDS 765 and supplied by Exciton. This setup resulted in approximately 10 mJ/pulse, with a wavelength of 760.15 nm, a linewidth of approximately 10 cm<sup>-1</sup>, and a repetition rate of 10 Hz. The 760.15 nm beam is focused with sheet forming optics ( $\approx 150 \mu\text{m}$  thickness) over the jet (Fig. 1 right, Fig. 2).

The timing is controlled by two pulse/delay generators. One pulse/delay generator (SRS DG535) is cycled internally at 10 Hz, and is used to trigger a second pulse/delay generator, and the flash lamps in the Nd:YAG lasers used to pump the dye lasers. The second pulse/delay generator (BNC 505-4C) is run in single shot mode and triggers the solenoid, the two Q-switches in the Nd:YAG lasers, and the gate for the intensified camera. The intensified camera is a Princeton Instruments PIMAX-2 1024x1024 with a 18 mm Gen III Extended Blue intensifier; the gain set to 255 for all experiments.

#### IV. Results

We present KTV results performed on an underexpanded jet for three cases of three mixtures: Case 1: 100% Kr, Case 2: 5%Kr/95% $\text{N}_2$ , and Case 3: 0.5% Kr/99.5%  $\text{N}_2$ . The underexpanded jet is pulsed, and after a fixed time delay, the krypton tracer is written. Then, the read sheet is pulsed at a further prescribed delay. This approach results in an observed distance of travel for the metastable krypton tracer for a specified time.

The conditions (Table 1) at the write location of the underexpanded jet are calculated with an empirical fit found in Crist et al.<sup>70</sup> That work gives a relation for the Mach number  $M$ , as a function of distance from the jet orifice  $x$ , jet diameter  $D_j$ , and ratio of specific heats  $\gamma$ . The velocity is found by calculating the sound speed at each corresponding Mach number from the isentropic gas relations.<sup>71</sup> The molecular weight and the ratio of specific heats for the mixtures are computed with Cantera.<sup>61</sup> A Case 4 is included in Table 1 to indicate a pure  $\text{N}_2$  jet and serve as a reference to quantify the alteration of transport properties.

For Case 1, we present KTV in a 100% krypton underexpanded jet. The metastable krypton tracer is written approximately two diameters from the jet orifice. The effective plenum pressure is approximately 240 kPa. A series of 15 exposures is presented as Fig. 3. The KTV exposure at 0  $\mu\text{s}$  (Fig. 3, top left) shows the jet boundary. The visualization of the boundary appears because the camera gate overlaps the read and write laser pulses. As the time delay between the read line and the write sheet is increased, there is an apparent translation of the tagged metastable Kr tracer. The decay in intensity of the spontaneous emission from the metastable Kr tracer is also apparent; this indicates that the metastable state is decaying and/or the number density of the tagged Kr is decreasing. Additionally, two dark points appear at the intersection of the jet boundary and the tagged metastable Kr tracer. At these two points, both the laser induced fluorescence and the spontaneous emission are being registered by the camera.

For Case 2, we present KTV of an underexpanded jet comprised of a 5%Kr/95% $\text{N}_2$  mixture. The metastable krypton tracer is written approximately two diameters from the jet orifice. The effective plenum pressure is approximately 180 kPa. A series of 10 exposures is presented as Fig. 4. In this series, the camera gate is chosen to bracket only the spontaneous emission from the metastable Kr tracer. This is apparent when comparing the image sequences in Fig. 3 and Fig. 4; that is, the laser induced fluorescence is not present at the bottom of each exposure in Fig. 4 because of the chosen camera gate.

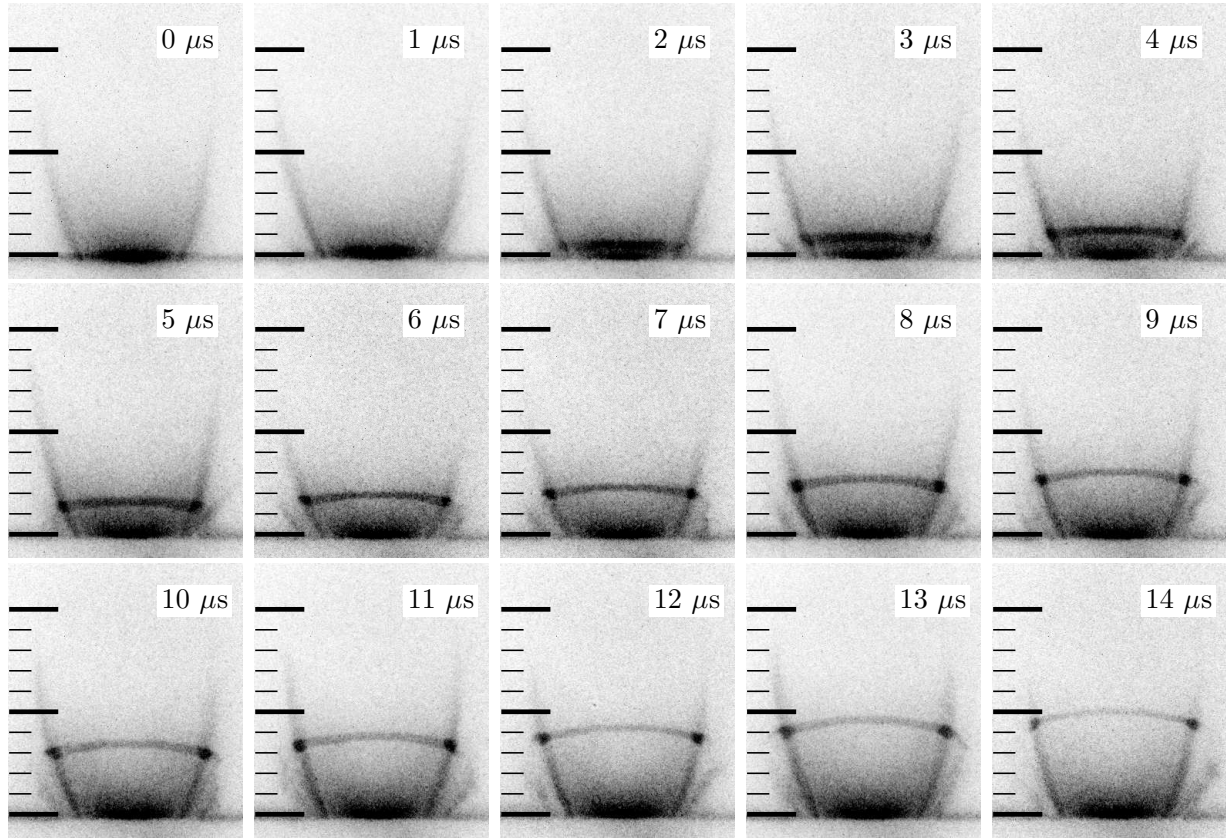


Figure 3. Case 1. KTV in a 100% krypton underexpanded jet. Inverted intensity scale. Conditions in Table 1. The camera gate is fixed to 20 $\mu$ s to include the write and read laser pulses. The time stamp of the delay between the write and read pulses is given in  $\mu$ s. Major tick marks are shown at 5 mm intervals.

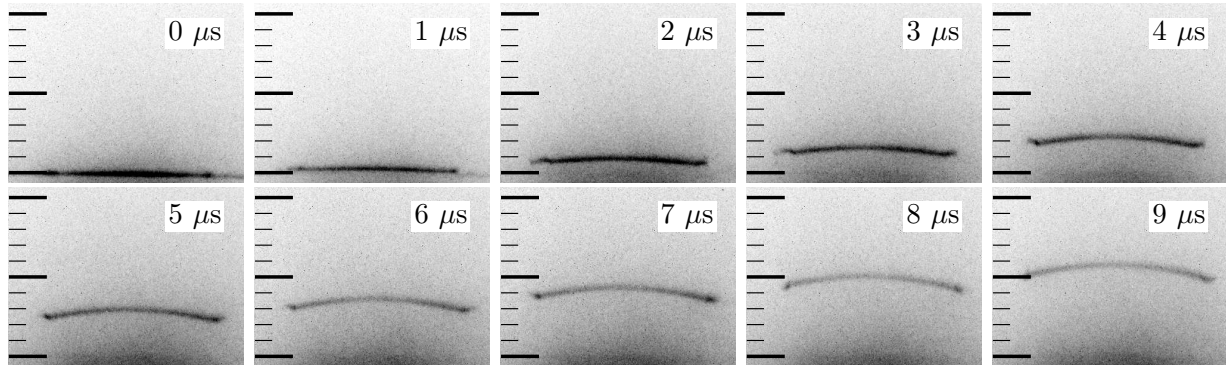


Figure 4. Case 2. KTV in a 5% Kr/95% N<sub>2</sub> underexpanded jet. Inverted intensity scale. Conditions in Table 1. The camera gate is fixed to include only the read laser pulses (after the first image). The time stamp of the delay between the write and read lines is given in  $\mu$ s. Major tick marks at 5 mm intervals.

For Case 3, we present KTV of an underexpanded jet comprised of a 0.5% Kr/99.5% N<sub>2</sub> mixture. The metastable krypton tracer is written approximately two diameters from the jet orifice. The effective plenum pressure is approximately 180 kPa. A series of 6 exposures is presented as Fig. 5. In this series, the camera gate is chosen to bracket only the spontaneous emission from the metastable Kr tracer.

## V. Analysis

A time-of-flight style analysis is used to calculate the one-dimensional velocity of the tagged metastable Kr tracer along the centerline of the underexpanded jet. In the interests of exploring the limits of the technique,

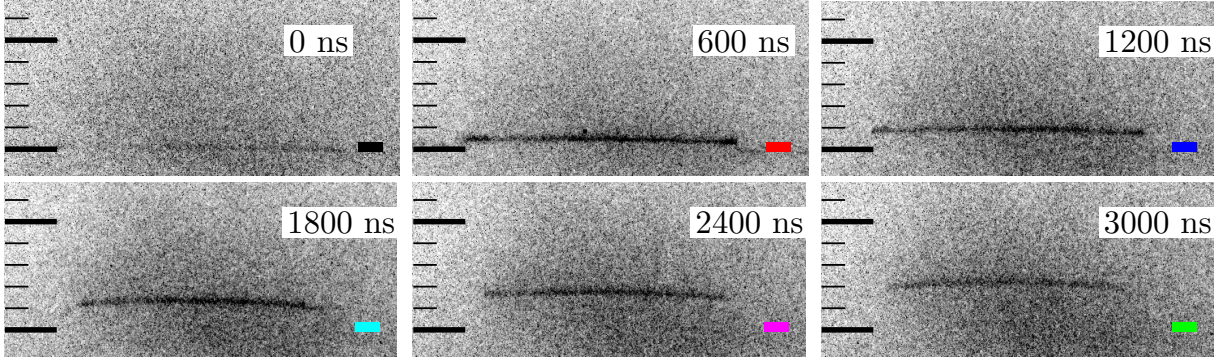


Figure 5. Case 3. KTV in a 0.5% Kr/99.5% N<sub>2</sub> underexpanded jet. Inverted intensity scale. Conditions in Table 1. The camera gate is fixed to include only the read laser pulses (after the first image). The time stamp of the delay between the write and read pulses is given in ns. Major tick marks are shown at 5 mm intervals. The color marks in the lower-right corner of each exposure correspond to the colors of the data presented in Fig. 6.

the 0.5% Kr/99.5% N<sub>2</sub> case will be analyzed because of its lower signal to noise ratio relative to the other experiments. The camera response is averaged along a 375  $\mu\text{m}$  (10 pixel) slice on the centerline to track the tagged krypton (left to right in each exposure of Fig. 5). The slice width is less than 1% of the radius of curvature of the tagged metastable Kr (computed by image processing in MATLAB); thus, two-dimensional effects need not be considered.

To find the center of mass location of the tagged metastable Kr, a Gaussian model of the form  $f(x) = a \exp(-((x - b)/c)^2)$  is fitted to the image intensity data, and  $b$  (the centroid) and the 95% confidence bounds are determined for each image intensity vector. The traversed distance,  $\Delta x$ , is then found (read-centroid location relative to the write-centroid location). Gaussian fits (solid lines) and the experimental data (diamond markers) are presented as Fig. 6 (left). Each centroid is marked with a circle, and the color of each plot corresponds to the color-mark in the lower right of each image in Fig. 5; for example, the write-location (black) and a read location (green) were determined from the intensity data in Fig. 6 (left), and these correspond to the upper-left, and lower-right images in Fig. 5 at 0 ns and 3000 ns, respectively. The time of flight,  $\Delta t$ , is the prescribed delay between the write and read laser Q-switch pulses.

Velocity is then found as  $V = \Delta x / \Delta t$  (Fig. 6, right); implicit in this formulation is that the local acceleration is small. The velocities presented in Fig. 6 (right) are plotted with the corresponding colors to Fig. 6 (left) and the lower-right corner of each exposure in Fig. 5. The velocity data appearing in Fig. 6 (right) denoted by thin black markers are from the same data set, but are omitted from Fig. 6 (left) and Fig. 5 for clarity.

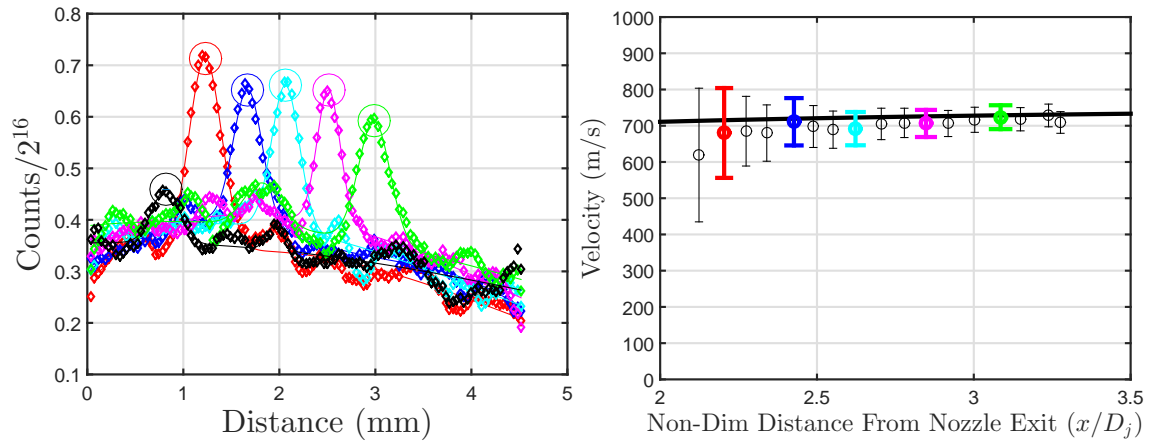


Figure 6. Left: Processed data from exposures in Fig. 5. Colors marking the processed image data correspond to the color marks in the lower right corner of each exposure in Fig. 5. The image intensity vectors are denoted by diamond markers, and the Gaussian fits to the data are marked by solid lines of the same color. The circles mark the centroid of the intensity data. Right: KTV in a 0.5% Kr/99.5% N<sub>2</sub> underexpanded jet. The circular markers are experimental KTV data, and the solid line is an empirical fit from Crist et al.<sup>70</sup>

of the data-reduction presentation.

The uncertainty in the experimental velocimetry results in Fig. 6 (right) is determined in the usual manner.<sup>72</sup> The uncertainty in  $\Delta x$  is estimated as the 95% confidence bound around the Gaussian centroid determined for each vector of image intensity. The uncertainty in  $\Delta t$  is estimated to be 50 ns; this estimate includes the uncertainty due to laser jitter and fluorescence blurring, as considered in Bathel et al.<sup>29</sup> Additionally, the uncertainty due to the predicted local acceleration of the gas (3%) is included in a root-means-squares sense. As expected, due to the functional form of the velocity relation ( $V = \Delta x / \Delta t$ ), the magnitude of the error bars decrease with distance from the non-dimensional distance from the write-line location. The uncertainty in the velocimetry results is below 5% at non-dimensional distances of greater than  $x/D_j \approx 2.75$ . These values of uncertainty are indicative of a strength of the KTV technique: the metastable Kr state is relatively long lived, which drives the velocimetry uncertainty down (assuming no local acceleration).

The experimental KTV results are compared to an empirical fit of an underexpanded jet found in Crist et al.<sup>70</sup> That work gives a relation for the Mach number  $M$ , as a function of distance from the jet orifice  $x$ , jet diameter  $D_j$ , and ratio of specific heats  $\gamma$ . The empirical fit is plotted as a solid line in Fig. 6 (right), and is found to fall within the error bars of the KTV results.

## VI. Conclusion

In this work, krypton tagging velocimetry (KTV) is performed in an underexpanded jet. The experimental setup and excitation scheme of krypton as a metastable tracer for velocimetry are presented. The data reduction scheme is described, and the uncertainty is estimated. A comparison of the experimental velocimetry data found with the KTV technique is compared to an empirical fit found in Crist et al.<sup>70</sup> The error bars are found to bound the empirical fit.

We demonstrate that the KTV technique can be employed in gas mixtures with relatively low krypton concentration (0.5% Kr/99.5% N<sub>2</sub>). Importantly, the uncertainty in the velocimetry results was found to be less than 5% for times of flight ( $\Delta t$ ) shorter than the metastable decay time. Additionally, the uncertainty in the velocimetry results could be reduced with refined treatment of the experimental setup. We conclude that the KTV technique shows promise as a velocimetry tool with krypton as an inert, dilute, long-lifetime tracer in gas-phase flows.

## Acknowledgments

The ASEE and the Air Force SFFP supported Parziale with a stipend for this work. The facilities and equipment were supplied by the Arnold Engineering Development Center. We would also like to acknowledge Joseph Wehrmeyer at Aerospace Testing Alliance (AEDC) for providing some of the laser systems.

## References

- <sup>1</sup>Tropea, C., Yarin, A. L., and Foss, J. F., *Springer Handbook of Experimental Fluid Mechanics*, Springer, 2007.
- <sup>2</sup>Koochesfahani, M. M. and Nocera, D. G., "Molecular Tagging Velocimetry," *Springer Handbook of Experimental Fluid Mechanics*, edited by Tropea, C. and Yarin, A. L. and Foss, J. F., Springer, 2007.
- <sup>3</sup>NCFMF, "National Committee for Fluid Mechanics Films," <http://web.mit.edu/hml/nccmf.html>.
- <sup>4</sup>Miles, R., Cohen, C., Connors, J., Howard, P., Huang, S., Markovitz, E., and Russell, G., "Velocity measurements by vibrational tagging and fluorescent probing of oxygen," *Optics Letters*, Vol. 12, No. 11, 1987, pp. 861–863. doi: [10.1364/OL.12.000861](https://doi.org/10.1364/OL.12.000861).
- <sup>5</sup>Miles, R., Connors, J., Markovitz, E., Howard, P., and Roth, G., "Instantaneous profiles and turbulence statistics of supersonic free shear layers by Raman excitation plus laser-induced electronic fluorescence (RELIEF) velocity tagging of oxygen," *Experiments in Fluids*, Vol. 8, No. 1-2, 1989, pp. 17–24. doi: [10.1007/BF00203060](https://doi.org/10.1007/BF00203060).
- <sup>6</sup>Miles, R. B., Zhou, D. B., Z., and Lempert, W. R., "Fundamental Turbulence Measurements by RELIEF Flow Tagging," *AIAA Journal*, Vol. 31, No. 3, 1993, pp. 447–452. doi: [10.2514/3.11350](https://doi.org/10.2514/3.11350).
- <sup>7</sup>B., M. R. and Lempert, W. R., "Quantitative Flow Visualization in Unseeded Flows," *Annual Review of Fluid Mechanics*, Vol. 29, No. 1, 1997, pp. 285–326. doi: [10.1146/annurev.fluid.29.1.285](https://doi.org/10.1146/annurev.fluid.29.1.285).
- <sup>8</sup>Miles, R. B., Grinstead, J., Kohl, R. H., and Diskin, G., "The RELIEF flow tagging technique and its application in engine

testing facilities and for helium-air mixing studies," *Measurement Science and Technology*, Vol. 11, No. 9, 2000, pp. 1272–1281. doi: [10.1088/0957-0233/11/9/304](https://doi.org/10.1088/0957-0233/11/9/304).

<sup>9</sup>Pitz, R. W., Brown, T. M., Nandula, S. P., Skaggs, P. A., DeBarber, P. A., Brown, M. S., and Segall, J., "Unseeded velocity measurement by ozone tagging velocimetry," *Optics Letters*, Vol. 21, No. 10, 1996, pp. 755–757. doi: [10.1364/OL.21.000755](https://doi.org/10.1364/OL.21.000755).

<sup>10</sup>Ribarov, L. A., Wehrmeyer, J. A., Batliwala, F., Pitz, R. W., and DeBarber, P. A., "Ozone Tagging Velocimetry Using Narrowband Excimer Lasers," *AIAA Journal*, Vol. 37, No. 6, 1999, pp. 708–714. doi: [10.2514/2.799](https://doi.org/10.2514/2.799).

<sup>11</sup>Pitz, R. W., Wehrmeyer, J. A., Ribarov, L. A., Oguss, D. A., Batliwala, F., DeBarber, P. A., Deusch, S., and Dimotakis, P. E., "Unseeded molecular flow tagging in cold and hot flows using ozone and hydroxyl tagging velocimetry," *Measurement Science and Technology*, Vol. 11, No. 9, 2000, pp. 1259–1271. doi: [10.1088/0957-0233/11/9/303](https://doi.org/10.1088/0957-0233/11/9/303).

<sup>12</sup>Michael, J. B., Edwards, M. R., Dogariu, A., and Miles, R. B., "Femtosecond laser electronic excitation tagging for quantitative velocity imaging in air," *Applied Optics*, Vol. 50, No. 26, 2011, pp. 5158–5162. doi: [10.1364/AO.50.005158](https://doi.org/10.1364/AO.50.005158).

<sup>13</sup>Dam, N., Klein-Douwel, R. J. H., Sijtsema, N. M., and ter Meulen, J. J., "Nitric oxide flow tagging in unseeded air," *Optics Letters*, Vol. 26, No. 1, 2001, pp. 36–38. doi: [10.1364/OL.26.000036](https://doi.org/10.1364/OL.26.000036).

<sup>14</sup>Sijtsema, N. M., Dam, N. J., Klein-Douwel, R. J. H., and ter Meulen, J. J., "Air Photolysis and Recombination Tracking: A New Molecular Tagging Velocimetry Scheme," *AIAA Journal*, Vol. 40, No. 6, 2002, pp. 1061–1064. doi: [10.2514/2.1788](https://doi.org/10.2514/2.1788).

<sup>15</sup>Van der Laan, W. P. N., Tolboom, R. A. L., Dam, N. J., and ter Meulen, J. J., "Molecular tagging velocimetry in the wake of an object in supersonic flow," *Experiments in Fluids*, Vol. 34, No. 4, 2003, pp. 531–534. doi: [10.1007/s00348-003-0593-1](https://doi.org/10.1007/s00348-003-0593-1).

<sup>16</sup>Krüger, S. and Grünefeld, G., "Stereoscopic flow-tagging velocimetry," *Applied Physics B*, Vol. 69, No. 5–6, 1999, pp. 509–512. doi: [10.1007/s003400050844](https://doi.org/10.1007/s003400050844).

<sup>17</sup>Orlemann, C., Schulz, C., and Wolfrum, J., "NO-flow tagging by photodissociation of NO<sub>2</sub>. A new approach for measuring small-scale flow structures," *Chemical Physics Letters*, Vol. 307, No. 1, 1999, pp. 15–20. doi: [10.1016/S0009-2614\(99\)00512-6](https://doi.org/10.1016/S0009-2614(99)00512-6).

<sup>18</sup>Hsu, A. G., Srinivasan, R., Bowersox, R. D. W., and North, S. W., "Molecular Tagging Using vibrationally Excited Nitric Oxide in an Underexpanded Jet Flowfield," *AIAA Journal*, Vol. 47, No. 11, 2009, pp. 2597–2604. doi: [10.2514/1.39998](https://doi.org/10.2514/1.39998).

<sup>19</sup>Hsu, A. G., Srinivasan, R., Bowersox, R. D. W., and North, S. W., "Two-component molecular tagging velocimetry utilizing NO fluorescence lifetime and NO<sub>2</sub> photodissociation techniques in an underexpanded jet flowfield," *Applied Optics*, Vol. 48, No. 22, 2009, pp. 4414–4423. doi: [10.1364/AO.48.004414](https://doi.org/10.1364/AO.48.004414).

<sup>20</sup>Sánchez-González, R., Srinivasan, R., Bowersox, R. D. W., and North, S. W., "Simultaneous velocity and temperature measurements in gaseous flow fields using the VENOM technique," *Optics Letters*, Vol. 36, No. 2, 2011, pp. 196–198. doi: [10.1364/OL.36.000196](https://doi.org/10.1364/OL.36.000196).

<sup>21</sup>Sánchez-González, R., Bowersox, R. D. W., and North, S. W., "Simultaneous velocity and temperature measurements in gaseous flowfields using the vibrationally excited nitric oxide monitoring technique: a comprehensive study," *Applied Optics*, Vol. 51, No. 9, 2012, pp. 1216–1228. doi: [10.1364/AO.51.001216](https://doi.org/10.1364/AO.51.001216).

<sup>22</sup>Jiang, N., Nishihara, M., and Lempert, W. R., "Quantitative NO<sub>2</sub> molecular tagging velocimetry at 500 kHz frame rate," *Applied Physics Letters*, Vol. 97, No. 22, 2010, pp. 221103. doi: [10.1063/1.3522654](https://doi.org/10.1063/1.3522654).

<sup>23</sup>Jiang, N., Nishihara, M., and Lempert, W. R., "500 kHz NO<sub>2</sub> Molecular Tagging Velocimetry in a Mach 5 Wind Tunnel," *27TH AIAA Aerodynamics Measurement Technology and Ground Testing Conference*, AIAA-2010-4348, Chicago, Illinois, 2010. doi: [10.2514/6.2010-4348](https://doi.org/10.2514/6.2010-4348).

<sup>24</sup>Bathel, B. F., Johansen, C. T., Danehy, P. M., Inman, J. A., and Jones, S. B., "Hypersonic Boundary Layer Transition Measurements Using NO<sub>2</sub> → NO Photo-dissociation Tagging Velocimetry," *Proceedings of 41st AIAA Fluid Dynamics Conference and Exhibit*, AIAA-2011-3246, Honolulu, Hawaii, 2011. doi: [10.2514/6.2011-3246](https://doi.org/10.2514/6.2011-3246).

<sup>25</sup>ElBaz, A. M. and Pitz, R. W., "N<sub>2</sub>O molecular tagging velocimetry," *Applied Physics B*, Vol. 106, No. 4, 2012, pp. 961–969. doi: [10.1007/s00340-012-4872-5](https://doi.org/10.1007/s00340-012-4872-5).

<sup>26</sup>Inman, J. A., Danehy, P. M., Bathel, B. F., and Nowak, R. J., "Laser-Induced Fluorescence Velocity Measurements in Supersonic Underexpanded Impinging Jets," *Proceedings of 48th AIAA Aerospace Sciences Meeting and Exhibit*, AIAA-2010-1438, Orlando, Florida, 2010. doi: [10.2514/6.2010-1438](https://doi.org/10.2514/6.2010-1438).

<sup>27</sup>Bathel, B. F., Danehy, P. M., Inman, J. A., Jones, S. B., Ivey, C. B., and Goyne, C. P., "Multiple Velocity Profile Measurements in Hypersonic Flows Using Sequentially-Imaged Fluorescence Tagging," *Proceedings of 48th AIAA Aerospace Sciences Meeting Including the New Horizons Forum and Aerospace Exposition*, AIAA-2010-1404, Orlando, Florida, 2010. doi: [10.2514/6.2010-1404](https://doi.org/10.2514/6.2010-1404).

<sup>28</sup>Bathel, B. F., Danehy, P. M., Inman, J. A., Watkins, A. N., Jones, S. B., Lipford, W. E., and Z., G. K., "Hypersonic Laminar Boundary Layer Velocimetry with Discrete Roughness on a Flat Plate," *Proceedings of 40th AIAA Fluid Dynamics Conference and Exhibit*, AIAA-2010-4998, Chicago, Illinois, 2010. doi: [10.2514/6.2010-4998](https://doi.org/10.2514/6.2010-4998).

<sup>29</sup>Bathel, B. F., Danehy, P. M., Inman, J. A., Jones, S. B., Ivey, C. B., and Goyne, C. P., "Velocity Profile Measurements in Hypersonic Flows Using Sequentially Imaged Fluorescence-Based Molecular Tagging," *AIAA Journal*, Vol. 49, No. 9, 2011, pp. 1883–1896. doi: [10.2514/1.J050722](https://doi.org/10.2514/1.J050722).

<sup>30</sup>Sánchez-González, R., Bowersox, R. D. W., and North, S. W., "Vibrationally excited NO tagging by NO(A<sup>2</sup>Σ<sup>+</sup>) fluorescence and quenching for simultaneous velocimetry and thermometry in gaseous flows," *Optics Letters*, Vol. 39, No. 9, 2014, pp. 2771–2774. doi: [10.1364/OL.39.002771](https://doi.org/10.1364/OL.39.002771).

<sup>31</sup>Danehy, P. M., Mere, P., Gaston, M. J., O'Byrne, S., Palma, P. C., and Houwing, A. F. P., "Fluorescence Velocimetry of the Hypersonic, Separated Flow over a Cone," *AIAA Journal*, Vol. 39, No. 7, 2001, pp. 1320–1328. doi: [10.2514/2.1450](https://doi.org/10.2514/2.1450).

- <sup>32</sup>O'Byrne, S., Danehy, P. M., and Houwing, A. F. P., "Nonintrusive Temperature and Velocity Measurements in a Hypersonic Nozzle Flow," *Proceedings of 22nd AIAA Aerodynamic Measurement Technology and Ground Testing Conference*, AIAA-2002-2917, St. Louis, Missouri, 2002. doi: [10.2514/6.2002-2917](https://doi.org/10.2514/6.2002-2917).
- <sup>33</sup>Danehy, P. M., O'Byrne, S., Houwing, A. F. P., Fox, J. S., and Smith, D. R., "Flow-tagging Velocimetry for Hypersonic Flows using Fluorescence of Nitric Oxide," *AIAA Journal*, Vol. 41, No. 2, 2003, pp. 263–271. doi: [10.2514/2.1939](https://doi.org/10.2514/2.1939).
- <sup>34</sup>McDaniel, J. C., Hiller, B., and Hanson, R. K., "Simultaneous multiple-point velocity measurements using laser-induced iodine fluorescence," *Optics Letters*, Vol. 8, No. 1, 1983, pp. 51–53. doi: [10.1364/OL.8.000051](https://doi.org/10.1364/OL.8.000051).
- <sup>35</sup>Balla, R. J., "Iodine Tagging Velocimetry in a Mach 10 Wake," *AIAA Journal*, Vol. 51, No. 7, 2013, pp. 1–3. doi: [10.2514/1.J052416](https://doi.org/10.2514/1.J052416).
- <sup>36</sup>Lempert, W. R., Jiang, N., Sethuram, S., and Samimy, M., "Molecular Tagging Velocimetry Measurements in Supersonic Microjets," *AIAA Journal*, Vol. 40, No. 6, 2002, pp. 1065–1070. doi: [10.2514/2.1789](https://doi.org/10.2514/2.1789).
- <sup>37</sup>Lempert, W. R., Boehm, M., Jiang, N., Gimelshein, S., and Levin, D., "Comparison of molecular tagging velocimetry data and direct simulation Monte Carlo simulations in supersonic micro jet flows," *Experiments in Fluids*, Vol. 34, No. 3, 2003, pp. 403–411. doi: [10.1007/s00348-002-0576-7](https://doi.org/10.1007/s00348-002-0576-7).
- <sup>38</sup>Handa, T., Mii, K., Sakurai, T., Immura, K., Mizuta, S., and Ando, Y., "Study on supersonic rectangular microjets using molecular tagging velocimetry," *Experiments in Fluids*, Vol. 55, No. 5, 2014, pp. 1–9. doi: [10.1007/s00348-014-1725-5](https://doi.org/10.1007/s00348-014-1725-5).
- <sup>39</sup>Boedeker, L. R., "Velocity measurement by H<sub>2</sub>O photolysis and laser-induced fluorescence of OH," *Optics Letters*, Vol. 14, No. 10, 1989, pp. 473–475. doi: [10.1364/OL.14.000473](https://doi.org/10.1364/OL.14.000473).
- <sup>40</sup>Wehrmeyer, J. A., Ribarov, L. A., Oguss, D. A., and Pitz, R. W., "Flame Flow Tagging Velocimetry with 193-nm H<sub>2</sub>O Photodissociation," *Applied Optics*, Vol. 38, No. 33, 1999, pp. 6912–6917. doi: [10.1364/AO.38.006912](https://doi.org/10.1364/AO.38.006912).
- <sup>41</sup>Pitz, R. W., Lahr, M. D., Douglas, Z. W., Wehrmeyer, J. A., Hu, S., Carter, C. D., Hsu, K.-Y., Lum, C., and Koochesfahani, M. M., "Hydroxyl tagging velocimetry in a supersonic flow over a cavity," *Applied Optics*, Vol. 44, No. 31, 2005, pp. 6692–6700. doi: [10.1364/AO.44.006692](https://doi.org/10.1364/AO.44.006692).
- <sup>42</sup>Hiller, B., Booman, R. A., Hassa, C., and Hanson, R. K., "Velocity visualization in gas flows using laser-induced phosphorescence of biacetyl," *Review of Scientific Instruments*, Vol. 55, No. 12, 1984, pp. 1964–1967. doi: [10.1063/1.1137687](https://doi.org/10.1063/1.1137687).
- <sup>43</sup>Gendrich, C. P. and Koochesfahani, M. M., "A spatial correlation technique for estimating velocity fields using molecular tagging velocimetry (MTV)," *Experiments in Fluids*, Vol. 22, No. 1, 1996, pp. 67–77. doi: [Springer](https://doi.org/10.1007/s003480050123).
- <sup>44</sup>Gendrich, C. P., Koochesfahani, M. M., and Nocera, D. G., "Molecular tagging velocimetry and other novel applications of a new phosphorescent supramolecule," *Experiments in Fluids*, Vol. 23, No. 5, 1997, pp. 361–372. doi: [10.1007/s003480050123](https://doi.org/10.1007/s003480050123).
- <sup>45</sup>Stier, B. and Koochesfahani, M. M., "Molecular tagging velocimetry (MTV) measurements in gas phase flows," *Experiments in Fluids*, Vol. 26, No. 4, 1999, pp. 297–304. doi: [10.1007/s003480050292](https://doi.org/10.1007/s003480050292).
- <sup>46</sup>Zel'dovich, Y. B. and Raizer, Y. P., *Physics of Shock Waves and High-Temperature Hydrodynamic Phenomena*, Dover, 2002.
- <sup>47</sup>Hsu, A. G., Narayanaswamy, V., Clemens, N. T., and Frank, J. H., "Mixture fraction imaging in turbulent non-premixed flames with two-photon LIF of krypton," *Proceedings of the Combustion Institute*, Vol. 33, No. 1, 2011, pp. 759–766. doi: [10.1016/j.proci.2010.06.051](https://doi.org/10.1016/j.proci.2010.06.051).
- <sup>48</sup>Stalker, R. J., "Hypervelocity Aerodynamics with Chemical Nonequilibrium," *Annual Review of Fluid Mechanics*, Vol. 21, 1989, pp. 37–60. doi: [10.1146/annurev.fluid.21.1.37](https://doi.org/10.1146/annurev.fluid.21.1.37).
- <sup>49</sup>Hornung, H. G., "Experimental Hypervelocity Flow Simulation, Needs, Achievements and Limitations," *Proceedings of the First Pacific International Conference on Aero Sc. and Tech.*, Taiwan, 1993.
- <sup>50</sup>Holden, M. S., Wadhams, T. P., and Candler, G. V., "Experimental Studies in the LENS Shock Tunnel and Expansion Tunnel to Examine Real-Gas Effects in Hypervelocity Flows," *Proceedings of the 42nd AIAA Aerospace Sciences Meeting and Exhibit*, AIAA 2004-0916, Reno, Nevada, 2004. doi: [10.2514/6.2004-916](https://doi.org/10.2514/6.2004-916).
- <sup>51</sup>Johnson, H. B., Seipp, T. G., and Candler, G. V., "Numerical Study of Hypersonic Reacting Boundary Layer Transition on Cones," *Physics of Fluids*, Vol. 10, No. 13, 1998, pp. 2676–2685. doi: [10.1063/1.869781](https://doi.org/10.1063/1.869781).
- <sup>52</sup>Parziale, N. J., Shepherd, J. E., and Hornung, H. G., "Differential Interferometric Measurement of Instability in a Hypervelocity Boundary Layer," *AIAA Journal*, Vol. 51, No. 3, 2013, pp. 750–754. doi: [10.2514/1.J052013](https://doi.org/10.2514/1.J052013).
- <sup>53</sup>Jewell, J. S., Wagnild, R. M., Leyva, I. A., Candler, G. V., and Shepherd, J. E., "Transition Within a Hypervelocity Boundary Layer on a 5-Degree Half-Angle Cone in Air/CO<sub>2</sub> Mixtures," *51st AIAA Aerospace Sciences Meeting including the New Horizons Forum and Aerospace Exposition*, AIAA-2013-0523, Grapevine, Texas, 2013. doi: [10.2514/6.2013-523](https://doi.org/10.2514/6.2013-523).
- <sup>54</sup>Buxton, O. R. H., Burns, R. A., and Clemens, N. T., "Simultaneous Krypton PLIF, LII and PIV Measurements in a Sooting Jet Flame," *Proceedings of 51st AIAA Aerospace Sciences Meeting including the New Horizons Forum and Aerospace Exposition*, AIAA-2013-0479, Grapevine, Texas, 2013. doi: [10.2514/6.2013-479](https://doi.org/10.2514/6.2013-479).
- <sup>55</sup>Velazco, J. E., Kolts, J. H., and Setser, D. W., "Rate constants and quenching mechanisms for the metastable states of argon, krypton, and xenon," *The Journal of Chemical Physics*, Vol. 69, No. 10, 1978, pp. 4357–4373. doi: [10.1063/1.436447](https://doi.org/10.1063/1.436447).
- <sup>56</sup>Katori, H. and Shimizu, F., "Lifetime measurement of the 1s<sub>5</sub> metastable state of argon and krypton with a magneto-optical trap," *Physical Review Letters*, Vol. 70, 1993, pp. 3545–3548. doi: [10.1103/PhysRevLett.70.3545](https://doi.org/10.1103/PhysRevLett.70.3545).
- <sup>57</sup>Lefers, J., Miller, N., Rupke, D., Tong, D., and Walhout, M., "Direct measurement of the metastable <sup>3</sup>P<sub>2</sub> decay rate in krypton," *Physical Review A*, Vol. 66, No. 1, 2002, pp. 012507. doi: [10.1103/PhysRevA.66.012507](https://doi.org/10.1103/PhysRevA.66.012507).
- <sup>58</sup>Mills, J. L., Sukenik, C. I., and Balla, R. J., "Hypersonic Wake Diagnostics Using Laser Induced Fluorescence Techniques," *Proceedings of 42nd AIAA Plasmadynamics and Lasers Conference*, AIAA 2011-3459, Honolulu, Hawaii, 2011. doi: [10.2514/6.2011-3459](https://doi.org/10.2514/6.2011-3459).

- <sup>59</sup>Balla, R. J. and Everhart, J. L., "Rayleigh Scattering Density Measurements, Cluster Theory, and Nucleation Calculations at Mach 10," *AIAA Journal*, Vol. 50, No. 3, 2012, pp. 698–707. doi: [10.2514/1.J051334](https://doi.org/10.2514/1.J051334).
- <sup>60</sup>Narayanaswamy, V., Burns, R., and Clemens, N. T., "Kr-PLIF for scalar imaging in supersonic flows," *Optics Letters*, Vol. 36, No. 21, 2011, pp. 4185–4187. doi: [10.1364/OL.36.004185](https://doi.org/10.1364/OL.36.004185).
- <sup>61</sup>Goodwin, D. G., "An Open-Source, Extensible Software Suite for CVD Process Simulation," *Proceedings of CVD XVI and EuroCVD Fourteen, M Allendorf, F Maury, and F Teyssandier (Eds.)*, 2003, pp. 155–162.
- <sup>62</sup>McBride, B. J., Zehe, M. J., and Gordon, S., "NASA Glenn Coefficients for Calculating Thermodynamic Properties of Individual Species," NASA TP-2002-211556, 2002.
- <sup>63</sup>Hirschfelder, J. O., Curtiss, C. F., and Bird, R. B., *Molecular Theory of Gases and Liquids*, John Wiley and Sons, 1954.
- <sup>64</sup>McQuarrie, D., *Statistical Mechanics*, University Science Books, 2000.
- <sup>65</sup>Miller, J. C., "Two-photon resonant multiphoton ionization and stimulated emission in krypton and xenon," *Physical Review A*, Vol. 40, 1989, pp. 6969–6976. doi: [10.1103/PhysRevA.40.6969](https://doi.org/10.1103/PhysRevA.40.6969).
- <sup>66</sup>Fonseca, V. and Campos, J., "Absolute transition probabilities of some Kr I lines," *Physica B+C*, Vol. 97, No. 2, 1979, pp. 312–314. doi: [10.1016/0378-4363\(79\)90064-0](https://doi.org/10.1016/0378-4363(79)90064-0).
- <sup>67</sup>Chang, R. S. F., Horiguchi, H., and Setser, D. W., "Radiative lifetimes and twobody collisional deactivation rate constants in argon for Kr(4p<sup>5</sup>5p) and Kr(4p<sup>5</sup>5p) states," *The Journal of Chemical Physics*, Vol. 73, No. 2, 1980, pp. 778–790. doi: [10.1063/1.440185](https://doi.org/10.1063/1.440185).
- <sup>68</sup>Whitehead, C. A., Pournasr, H., Bruce, M. R., Cai, H., Kohel, J., Layne, W. B., and Keto, J. W., "Deactivation of twophoton excited Xe(5p<sup>5</sup>6p,6p',7p) and Kr(4p<sup>5</sup>5p) in xenon and krypton," *The Journal of Chemical Physics*, Vol. 102, No. 5, 1995, pp. 1965–1980. doi: [10.1063/1.468763](https://doi.org/10.1063/1.468763).
- <sup>69</sup>Dzierżga, K., Volz, U., Nave, G., and Griesmann, U., "Accurate transition rates for the 5p-5s transitions in Kr I," *Physical Review A*, Vol. 62, No. 2, 2000, pp. 022505. doi: [10.1103/PhysRevA.62.022505](https://doi.org/10.1103/PhysRevA.62.022505).
- <sup>70</sup>Crist, S., Glass, D. R., and Sherman, P. M., "Study of the Highly Underexpanded Sonic Jet," *AIAA Journal*, Vol. 4, No. 1, 1966, pp. 68–71. doi: [10.2514/3.3386](https://doi.org/10.2514/3.3386).
- <sup>71</sup>Liepmann, H. W. and Roshko, A., *Elements of Gasdynamics*, John Wiley and Sons, Inc., 1957.
- <sup>72</sup>Moffat, R. J., "Describing the Uncertainties in Experimental Results," *Experimental Thermal and Fluid Science*, Vol. 1, No. 1, 1988, pp. 3–17. doi: [10.1016/0894-1777\(88\)90043-X](https://doi.org/10.1016/0894-1777(88)90043-X).